Sorting signals recorded during EDX experiments

Sadeg Said, Jean Cauzid, Cécile Fabre, El-Hadi Djermoune

Sorting Signals Recorded During EDX Experiments

Sadeg Said*, Jean Cauzid*, Cecile Fabre*, El-Hadi Djermoune**

*GeoRessources, Université de Lorraine, CNRS, F-54000 Nancy, France
**CRAN, Université de Lorraine, CNRS, F-54000 Nancy, France

Goal

The objective of this work is to separate the various signals recorded by the detectors of a Bruker Tornado M4 μXRF analyzer. That device is dedicated to the micro-imaging of the elements in solid samples. The work is conducted on a thin section from the Saint Mélany deposit in the French Massif Central. That sample hosts cassiterite and wolframite macro-crystals surrounded by quartz.

Introduction

XRF provides the elemental composition of a sample. The EDX detector used in our setup records all X-rays emerging from the sample. XRF stricto sensu corresponds to the specific emission lines of the atoms in the sample. However, the sample can also scatter the signal from the X-ray tube itself. Three scattering signals occur: elastic and inelastic scattering of the specific emission lines of the tube material, elastic and inelastic scattering of the bremsstrahlung and coherent elastic scattering from the periodic atomic organization in crystals. The first scattering manifests as extra peaks (Compton and Rayleigh) on the recorded spectrum, the second as a baseline and the third as X-ray diffraction peaks. These spectra are superimposed with XRF stricto sensu. Each of these four signals contain useful geochemical information.

Baseline Processing

In order to extract the baseline part from a fluorescence spectrum, we used several algorithms and selected the one providing the best fitting accuracy (Fig. 1). The algorithms we used include ASPLS [6], IRSQ [1], SNIP [5], MORMOL [2], PSALSA [4], and quantile regression [3].

Diffraction Peaks Processing

Once the baseline signal is removed, the diffraction peaks are processed using two methods, both exploiting the signals captured by the two detectors of the XRF analyzer. Method 1 estimates the position of the peaks in the spectrum corresponding to the difference between the two measured signals. The peaks that do not appear in one of the two original spectra (using a fixed threshold) are then classified as diffraction peaks. Method 2 computes and compares all the peak positions and widths appearing in the two recorded spectra to generate the list of diffraction peaks. The second method is clearly more costly in computation time than the first.

Conclusion

In this work we tested several methods for baseline extraction and compared the results using clustering to determine how much information was retained in the signal. We then moved on to the processing of diffraction peaks and evaluated two methods to clean up the signal: the second method was much better than the first but it is more costly. As a future work, we will focus on the Campton and Rayleigh peaks working on a half drill core.

Contact Information

- said.sadeg@univ-lorraine.fr
- el-hadi.djermoune@univ-lorraine.fr
- jean.cauzid@univ-lorraine.fr
- cecile.fabre@univ-lorraine.fr

[1] Q. Han, S. Peng, Q. Xie, Y. Wu, and G. Zhang. Iterative reweighted quantile regression using augmented lagrangian optimization for baseline correction. In *2018 5th International Conference on Information Science and Control Engineering (ICISCE)*, pages 280–284, Los Alamitos, CA, USA, July 2018. IEEE Computer Society. doi: 10.1109/ICISCE.2018.00066. URL https://doi.ieeecomputersociety.org/10.1109/ICISCE.2018.00066.

[2] M. Koch, C. Suhr, B. Roth, and M. Meinhardt-Wollweber. Iterative morphological and mollifier-based baseline correction for Raman spectra. *Journal of Raman Spectroscopy*, 48(2):336–342, 2017. doi: https://doi.org/10.1002/jrs.5010. URL https://analyticalsciencejournals.onlinelibrary.wiley.com/doi/abs/10.1002/jrs.5010.

[3] Ł. Komsta. Comparison of several methods of chromatographic baseline removal with a new approach based on quantile regression. *Chromatographia*, 73(7): 721–731, 2011. doi: 10.1007/s10337-011-1962-1. URL https://doi.org/10.1007/s10337-011-1962-1.

[4] S. Oller-Moreno, A. Pardo, J. M. Jiménez-Soto, J. Samitier, and S. Marco. Adaptive asymmetric least squares baseline estimation for analytical instruments. In *IEEE 11th International Multi-Conference on Systems, Signals Devices (SSD14)*, pages 1–5, 2014. doi: 10.1109/SSD.2014.6808837.

[5] C. G. Ryan, E. Clayton, W. L. Griffin, S. H. Sie, and D. R. Cousens. SNIP, a statistics-sensitive background treatment for the quantitative analysis of PIXE spectra in geoscience applications. *Nuclear Instruments and Methods in Physics Research B*, 34(3):396–402, Sept. 1988. doi: 10.1016/0168-583X(88)90063-8. URL https://ui.adsabs.harvard.edu/abs/1988NIMPB..34..396R.

[6] F. Zhang, X. Tang, A. Tong, B. Wang, J. Wang, Y. Lv, C. Tang, and J. Wang. Baseline correction for infrared spectra using adaptive smoothness parameter penalized least squares method. *Spectroscopy Letters*, 53(3):222–233, 2020. doi: 10.1080/00387010.2020.1730908. URL https://doi.org/10.1080/00387010.2020.1730908.

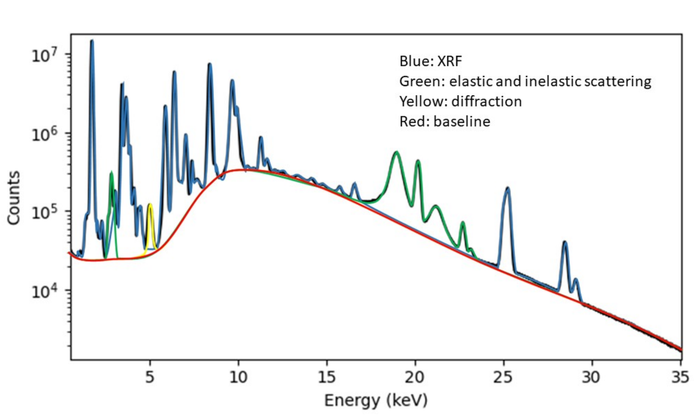

Fig 1. composition of spectrum

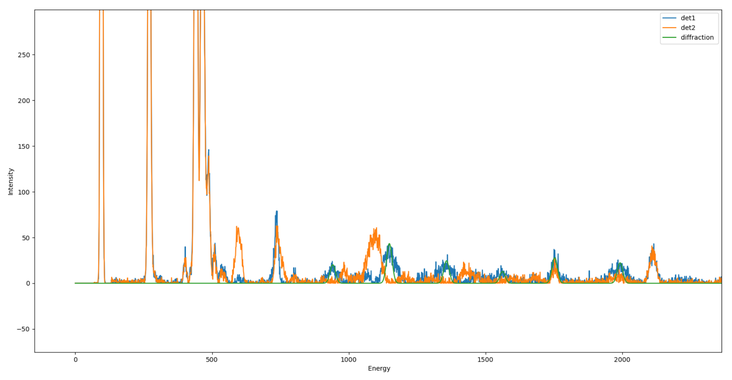

Fig 2. Fitted diffraction peaks found by Method 1

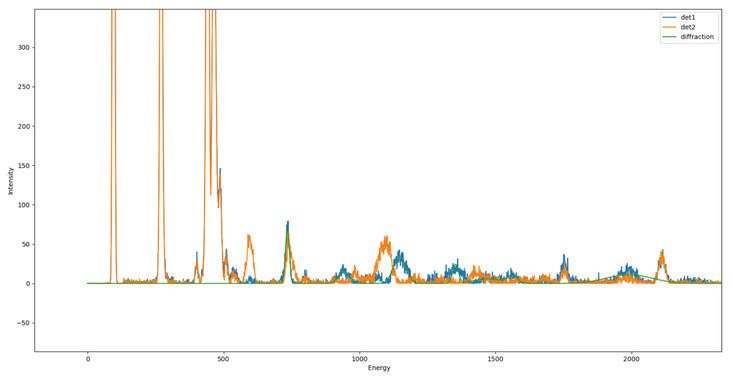

Fig 3. Fitted diffraction peaks found by Method 2

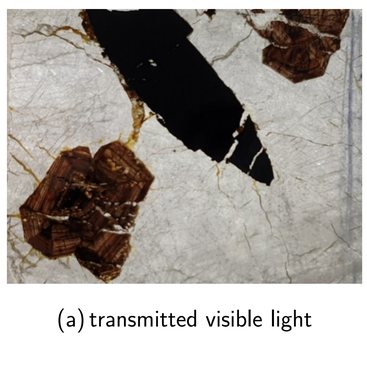

(a) transmitted visible light

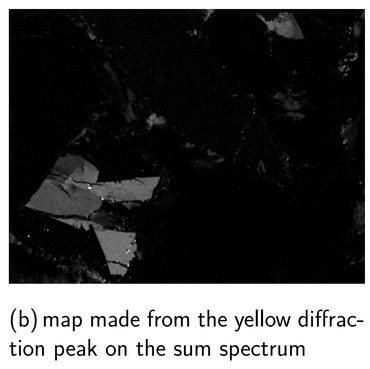

(b) map made from the yellow diffraction peak on the sum spectrum

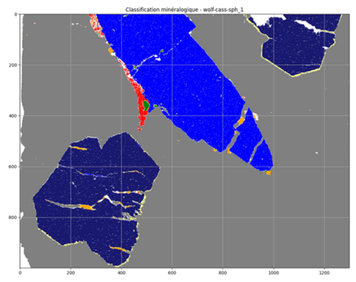

(c) minerals classified from XRF signal (blue peaks on the sum spectrum).

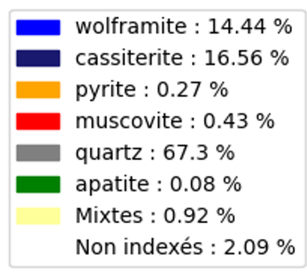

(d) proportion of each mineral in the map

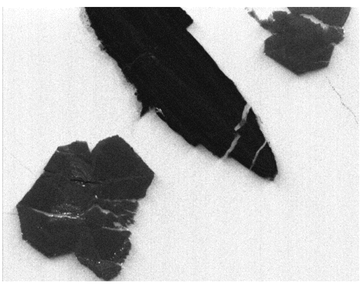

(e) map made from the inelastic scattering peaks (part of the green peaks on sum spectrum)

Fig 4.different maps showing the sample